



Yao, J., Yang, W., Gao, Y., Scarpa, F., & Li, Y. (2019).  
Magnetorheological elastomers with particle chain orientation:  
Modelling and experiments. *Smart Materials and Structures*, 28(9).  
<https://doi.org/10.1088/1361-665X/ab2e21>

Peer reviewed version

License (if available):  
CC BY-NC-ND

Link to published version (if available):  
[10.1088/1361-665X/ab2e21](https://doi.org/10.1088/1361-665X/ab2e21)

[Link to publication record in Explore Bristol Research](#)  
PDF-document

This is the accepted author manuscript (AAM). The final published version (version of record) is available online via IOP Publishing at <https://iopscience.iop.org/article/10.1088/1361-665X/ab2e21> . Please refer to any applicable terms of use of the publisher.

## University of Bristol - Explore Bristol Research

### General rights

This document is made available in accordance with publisher policies. Please cite only the published version using the reference above. Full terms of use are available:  
<http://www.bristol.ac.uk/red/research-policy/pure/user-guides/ebr-terms/>

# Magnetorheological Elastomers with Particle Chain Orientation: Modelling and Experiments

Jianfei Yao<sup>a,b,c</sup>, Wei Yang<sup>a,c</sup>, Yu Gao<sup>b,c</sup>, Fabrizio Scarpa<sup>d</sup>, Yan Li<sup>a,b</sup>

<sup>a</sup> Beijing Key Laboratory of Health Monitoring and Self-recovering for High-end Mechanical Equipment, Beijing University of Chemical Technology, Beijing, 100029, China

<sup>b</sup> Key Lab of Engine Health Monitoring-Control and Networking of Ministry of Education, Beijing University of Chemical Technology, Beijing, 100029, China

<sup>c</sup> College of Mechanical and Electrical Engineering, Beijing University of Chemical Technology, Beijing, 100029, China

<sup>d</sup> Bristol Composites Institute (ACCIS), University of Bristol, Bristol BS8 1TR, UK

(Corresponding author: Jianfei Yao, Email: yaojf@mail.buct.edu.cn)

Received xxxxxx

Accepted for publication xxxxxx

Published xxxxxx

## Abstract

This work describes a new model of the magneto-induced shear storage modulus to simulate the shear behavior of magnetorheological elastomers (MRE) with particle chain orientation. The directionality of the chains is here described by using as a parameter the tilt angle with the external magnetic field. The magnetized particles within the MRE are described as magnetic dipoles. The model takes into consideration the dipole-dipole interaction and the magnetic field coupling between the particles in the chain. Magneto-rheological samples with different particle sizes and initial inclination angles have also been prepared and subjected to shear tests in a rheometer facility. The simulations from the model show that the magneto-induced modulus strongly depends on the initial inclination angle of the particle chain. The experimental data are also consistent with the results provided by the model, and confirm that the change of the initial tilt angle of the particle chain is an effective tool to improve the mechanical properties of magneto-rheological elastomers.

Keywords: Magnetorheological elastomer, Chain structure orientation, Magnetic dipole, Magneto-induced shear modulus

## 1. Introduction

Magnetorheological elastomers (MREs) consist of micron-sized soft magnetic particles embedded in a polymer matrix. MRE is a type of smart composite that combines the advantages of magnetorheological materials and elastomeric solids. Compared to magnetorheological fluids, MREs possess good mechanical and rheological stability due to the absence of particle sedimentation. MREs also exhibit controllable magnetic, mechanical and electrical properties when subjected to an external magnetic field [1-2]; and these characteristics of MREs, such as stiffness and damping, are exploited in a variety of engineering applications [3-8]. The stiffness of MREs is proportional to their storage modulus, which depends upon the initial modulus at zero magnetic field and the magnetic modulus caused by the operated magnetic field [9-10]. The magneto-induced modulus is an important index to measure the range of

the change of stiffness. It is nonetheless necessary to consider how the various material parameters affect theoretically the magneto-induced modulus to design high-performance MREs. Most studies focused on the mechanical performance of MREs are dedicated to the modification of soft magnetic particles and the selection of matrix materials [11-14]. The magneto-induced mechanical properties of MREs are however also dependent upon the arrangement of these particles inside the matrix [15-17]. It is generally believed that anisotropic MREs possess a higher magneto-induced modulus than the isotropic magneto-rheological composites. The particles inside the matrix tend to arrange in a chain-like configuration in the pre-structure process when their volume fraction is small [18]. It is therefore quite necessary to establish a microscopic model of magneto-rheological elastomers to understand the influence of the particle chain arrangement on the mechanical properties of the

composite; this theoretical model could provide design guidelines to fabricate samples of high-performance MREs.

The MREs models described in open literature tend to make use of the magnetic dipole framework proposed by Jolly et al. [19]. The dipole approach simplifies the overall behavior of the ferromagnetic particles and allows to calculate the interaction energy between particles to obtain an expression of the magneto-induced modulus. Davis [20] has used the magnetic dipole theory to compare and analyze the mechanical behavior of matrices before and after the dispersion of ferromagnetic particles. Davis' model could predict the optimum volume fraction of particles and the maximum magneto-induced shear modulus in MRE. Shen et al. [21] have further developed Davis' approach by assuming that the particles form multiple chains, and have proposed a chain model based on the presence of a coupled field. Zhu et al. [22] have proposed a further modification of this approach by developing a chain adsorption model by considering that the length of the particle chain was not uniform. A magnetic dipole model based on a chi-squared distribution has been proposed by Suo Si by considering the distribution of the distance between adjacent particles [23]. All the models cited above consider the main factors affecting the magneto-induced mechanical properties of MREs from the micro-structure perspective.

Other studies have shown that the orientation of the particle chain also affects the magneto-induced properties of magneto-rheological elastomers. Yu et al. [24] assumed that the internal particle chain is not completely aligned with the direction of the applied magnetic field during the formation of the MRE architecture, but instead it possesses a specific angle with the direction of the field. In their work the authors analyzed the influence of the angle on the magneto-induced properties of the elastomer, however they did not perform any experimental verification. Boczkowska et al. [25-26] developed MREs with the same volume fraction and different particle alignment directions, and found that the structure of the micro-alignment of the particles plays a major role on the magnetorheological effect. Tian et al. [27] also found that magneto-rheological elastomers with a 45° angle between the particle chains and the direction of the external magnetic field possess a higher value of storage modulus in the specific direction than that in the contrary direction. Gao and Wang [28] predicted the existence of a negative magneto-induced modulus at a specific angle between the particle chain and the external magnetic field. All the studies cited above have demonstrated the importance of the orientation of the particle chain on the magneto-induced properties of magneto-rheological elastomers, however to the best of the Authors' knowledge no systematic theoretical or experimental explanation of this phenomenon has been proposed so far.

In this paper we develop a model to describe the magneto-induced modulus in MREs based on the use of magnetic dipoles theory and the knowledge of the initial angle between the particle chain and the external magnetic field. The model allows

to derive the magnetic dipole moment of the magnetized particles generated by the coupling with between magnetic field and the chain of particles. The variation of the interaction force between particles aligned along an initial angle of the chain is analyzed, and a micromechanical model of the magneto-induced shear storage modulus of the elastomer with the initial inclination of the particle chain is established. The model allows to predict the variation of the magneto-induced shear storage modulus of the MRE with the initial inclination of the particle chain. Silicone rubber-based MRE samples with five particle sizes (3-5μm, 10μm, 38μm, 75μm, 150μm) six different initial inclination angles (0°, 30°, 45°, 60°, 75°, 90°) and same mass fraction of 33% have been prepared. Observations from Scanning Electron Microscope (SEM) images show that the particles in the elastomers are arranged along an oblique chain structure. Rheometer (MCR301) tests show that the variation of the measured magneto-induced modulus with the initial inclination of the particle chain is consistent with the predictions provided by the proposed model. We also demonstrate that particle size is also an important factor to affect the magneto-induced mechanical properties of MREs. The initial inclination angle of the particle chain and the size of the particles are additional important parameters to design a magneto-rheological elastomer. The work presented here can provide theoretical guidelines for engineering and making high-performance MREs and their magneto-induced properties.

## 2. Modeling

### 2.1 The magnetic dipole moment

Magnetic particles are considered as magnetic dipoles after magnetization [29]. Under the action of an external magnetic field, ferromagnetic particles can be magnetized to induce a magnetic dipole moment  $\hat{m}$  with the same direction of the applied magnetic field. The magnetized particles then arrange in a chain structure along the direction of the external magnetic field. The spatial layout between any adjacent particles  $m_i$  and  $m_j$  when the angle between the particle chain and the applied magnetic field is  $\theta$ , is shown in Fig. 1. The magnetic field at a distance  $r$  from a magnetic dipole moment  $m$  is given by [30]:

$$\mathbf{B} = \frac{\mu_0}{4\pi} \left[ \frac{3(\hat{m} \cdot \hat{r})\hat{r}}{r^5} - \frac{\hat{m}}{r^3} \right] = \frac{\mu_0}{4\pi r^3} [3 \cos \theta \hat{r} - \hat{m}] \quad (1)$$

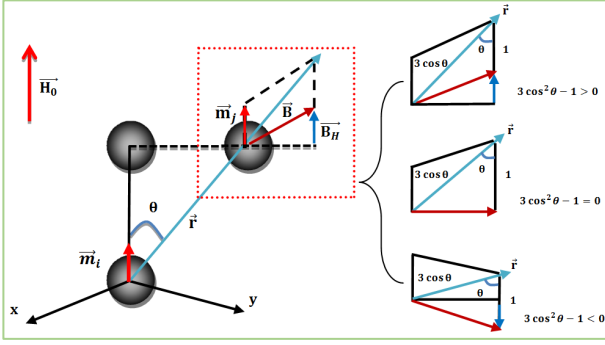


Figure 1 Layout of the interaction and geometry between two magnetic dipoles

In (1),  $\hat{r}$  and  $\hat{m}$  are the unit vectors along the direction of the radial axis  $\hat{r}$  and the applied magnetic field  $\hat{H}$ , respectively. From the inspection of Equation (1) it is possible to appreciate that the direction of the magnetic field created by the dipoles  $m_i$  at  $m_j$  is not along  $\hat{r}$ , but possesses a specific angle. The magnetic field created by the magnetic dipole  $m_i$  at  $m_j$  is  $\mathbf{B} = \frac{\mu_0 m}{4\pi r^3} \sqrt{1 + 3 \cos^2 \theta}$ . Its component along the direction of the applied magnetic field is  $B_H = \frac{\mu_0 m}{4\pi r^3} [3 \cos^2 \theta - 1]$ . The field  $\mathbf{B}$  is perpendicular to the applied magnetic field  $\mathbf{H}_0$  when  $3 \cos^2 \theta - 1 = 0$ , resulting in  $\theta \approx 54.74^\circ$ . When  $\theta < 54.74^\circ$  the magnetic field generated between particles has components along the same direction as the external magnetic field, however when  $\theta > 54.74^\circ$  the opposite is true. According to the coupling field theory proposed by Shen [21], particle interactions are present only on the same chain because other chains are located at long distances. The total magnetic field produced by particles present on the same chain is superimposed to the external magnetic field  $H_0$ . The magnetic field on any particle  $H_i$  can be therefore expressed as follows:

$$H_i = H_0 + \sum_{j \neq i} H_j = H_0 + 2 \cdot \sum_{j=1}^n \frac{(3 \cos^2 \theta - 1)m}{4\pi\mu_0\mu_l r_j^2} \quad (2)$$

Where  $H_0$  is the applied external magnetic field,  $H_j$  is the magnetic field created by the magnetization of the  $j^{\text{th}}$  dipole, and  $r_j$  is the spacing between particles. It is assumed here that the magnetic particles are uniform spheres, they are all located on the same chain and are equally spaced. If the distance between adjacent particles is  $r$ , then  $r_j = j \cdot r$  ( $j=1 \sim n$ ). The magnetic dipole moment of the particles in the chain is then expressed as:

$$\mathbf{r} = \frac{4}{3} \pi a^3 \mu_0 \mu_l \chi H_i \quad (3)$$

In (3)  $a$  is the particle radius,  $\chi$  is the susceptibility of the iron particles,  $H_i$  is the magnetic field strength at the  $i^{\text{th}}$  location of the chain,  $\mu_0$  is the permeability of the vacuum and  $\mu_l$  is the

permeability of the MR elastomer. If (2) is substituted into (3) one obtains :

$$m = \frac{4}{3} \pi a^3 \mu_0 \mu_l \chi \left[ H_0 + 2 \cdot \sum_{j=1}^n \frac{(3 \cos^2 \theta - 1)m}{4\pi\mu_l\mu_0 r_j^2} \right] \quad (4)$$

Developing Equation (4) one obtains:

$$m = \frac{4}{3} \pi a^3 \mu_0 \mu_l \chi H_0 \left[ \frac{1}{1 - 2C\chi \left(\frac{a}{r}\right)^3 \cos^2 \theta + \frac{2}{3} C\chi \left(\frac{a}{r}\right)^3} \right] \quad (5)$$

When the chain is very long the index  $n$  is large and the term  $C$  becomes  $C = \sum_{j=1}^n 1/j^3 \approx 1.2$ .

## 2.2 The interaction force between magnetic dipoles

The interaction between two magnetic dipoles  $\mathbf{m}_i$  and  $\mathbf{m}_j$  is shown in Fig. 2 The angle  $\theta$  is defined between the dipole  $\mathbf{m}_i$  and the distance vector  $\hat{r}$ ;  $\alpha$  is the angle between  $\mathbf{m}_j$  and  $\hat{r}$ , the angle  $\beta$  is defined between  $\mathbf{m}_i$  and  $\mathbf{m}_j$ . The energy interaction between the magnetic dipoles can be expressed as [29]:

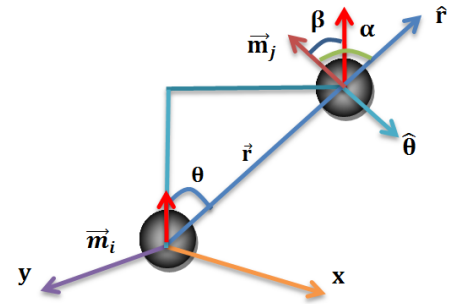


Figure 2 Interaction between two magnetic dipoles

$$E_{ij} = -\mathbf{m}_j \cdot \mathbf{B}_i = \frac{-m_i m_j}{4\pi\mu_0\mu_l r^3} [3 \cos \alpha \cos \theta - \cos \beta] \quad (6)$$

(6)

The interaction force between the magnetic dipoles is:

$$\mathbf{F} = -\nabla \left( -\mathbf{m}_j \cdot \mathbf{B}_i \right) = \frac{m_i m_j}{4\pi\mu_0\mu_l} \nabla \left[ \frac{3 \cos \alpha \cos \theta - \cos \beta}{r^3} \right] \quad (7)$$

(7)

When  $\beta = 0$  the angle  $\alpha$  becomes equal to  $\theta$ . In that specific case Equation (7) becomes:

$$\mathbf{F} = \frac{3m_i m_j}{4\pi\mu_0\mu_l r^4} \left[ (1 - 3 \cos^2 \theta) \hat{r} - (2 \cos \theta \sin \theta) \hat{\theta} \right] \quad (8)$$

In (8)  $\hat{r}$  represents the vector along the radial direction and  $\hat{\theta}$  is the angular direction vector. The angle  $\theta$  is the angle between the inter-particles vector and the direction of the

magnetic dipole moment. The variation of the radial and angular components of the interaction force versus is shown in Fig.3 (a). When the radial and angular components of the interaction force in the Fig.3 (a) shows a negative value, the force is opposite to the  $\hat{r}$  and  $\hat{\theta}$  directions at this specific angle. The vector equivalent of the diagram is shown in Fig. 3 (b).

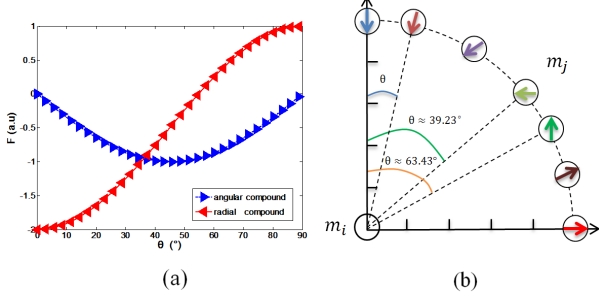


Figure 3 Angular dependence of the dipole-dipole force. (a) The red line indicates the radial force, while the blue line represents the angular one. (b) The force is plotted in a vector form for different positions of particle  $m_j$

The radial and the angular forces are combined to obtain the total horizontal interaction force of the two magnetic dipoles present in the same chain. The magnitude of this force equates to the shear force of the MRE when sheared [31]:

$$F = \frac{3m_i m_j}{4\pi\mu_0\mu_1 r^4} \left[ 2\cos^2\theta \sin\theta - (1-3\cos^2\theta)\sin\theta \right] \quad (9)$$

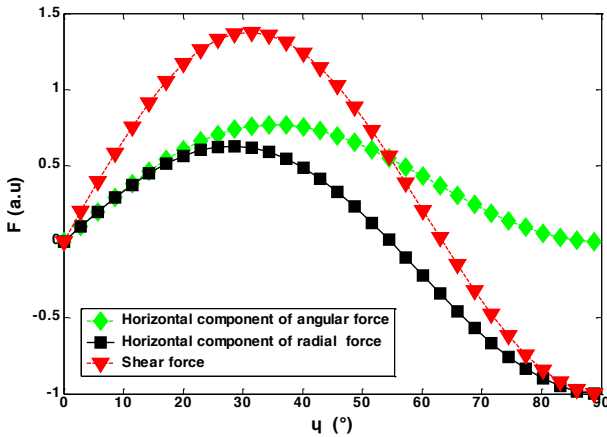


Figure 4 Horizontal components of the radial (black) and angular (green) forces. The shear force versus the chain angle is in red

Figure 4 shows the different horizontal components of the radial and angular forces, and the shear resultant versus the angle  $\theta$ . The shear force increases with increasing angles and then becomes smaller, indicating the presence of attraction interactions. At a specific the direction of the shear force changes, showing a repulsion behavior. If one considers all the particles interacting within the chain and that the magnetic dipole moments are equal ( $m_i = m_j$ ), the shear force can be expressed as:

$$F = \frac{3Am^2}{2\pi\mu_0\mu_1 r^4} \left[ 5\cos^2\theta \sin\theta - \sin\theta \right] \quad (10)$$

Where  $A = \sum_{i=1}^n 1/r^4 \approx 1.082$ .

### 2.3 Magneto-induced shear modulus

Magnetic particles can be represented as chains arranged within the microstructure of a magneto-rheological elastomer. A schematic of the arrangement between the particle chains and the neighboring magnetic dipoles before and after the shear deformation is shown in Fig. 5. The distance between adjacent particles along the direction of the external magnetic field is  $r_0$ ; the distance between particles before shear deformation is  $r_1$  and after deformation is  $r_2$ . The initial inclination angle is  $\theta$ , while the inclined chain strain angle is  $\delta$ . We indicate the magneto-induced shear storage modulus as  $\Delta G$ , and we consider the shear force uniformly distributed on each particle of the chain.

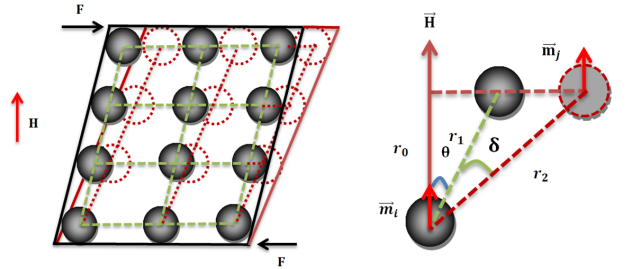


Figure 5 Arrangement of the particles before and after the shear deformation

An increase of the shear modulus  $\Delta G$  induced by the external magnetic fields is represented as :

$$\Delta G = nF/\gamma' \quad (11)$$

In (11),  $n$  is the number of particles in a unit cross section of the chain. The value of  $n$  is determined as :

$$n = \frac{3\phi r_0}{4\pi a^3} \quad (12)$$

Where  $\phi$  is the volume fraction of the particles in the MRE. The relationship between the shear strain  $\gamma'$  of the particle chain and the shear strain  $\gamma$  of the whole MRE is [32]

$$\gamma' = \gamma \cdot \cos^2\theta. \text{ The expression of the shear force is therefore:}$$

$$\Delta G = \frac{9\phi A r_0 \left[ 5\cos^2(\theta + \delta)\sin(\theta + \delta) - \sin(\theta + \delta) \right]}{8\pi^2 a^3 \mu_0 \mu_1 r_2^4 \gamma \cdot \cos^2\theta} m^2 \quad (13)$$

From the inspection of Figure 5 one can observe that  $\cos(\theta + \delta) = r_0/r_2$  and  $\cos\theta = r_0/r_1$ . If we denominate the parameter  $K$  as:

$$K = \frac{[5 \cos^2(\theta + \delta) - 1] \sin(\theta + \delta) \cdot \cos^4(\theta + \delta)}{\cos^2 \theta} \quad (14)$$

The final expression of the magneto-induced shear modulus is obtained by substituting (5) in (13):

$$\Delta G = \frac{2\phi A \mu_0 \mu_1 \left(\frac{a}{r_0}\right)^3 K}{\gamma} \cdot \left[ \frac{\chi H_0}{1 - 2C\chi \left(\frac{a}{r_0}\right)^3 \cos^5 \theta + \frac{2}{3} C\chi \left(\frac{a}{r_0}\right)^3 \cos^3 \theta} \right]^2 \quad (15)$$

Equation (15) shows that the magneto-induced modulus is not only related to the magnitude of the applied magnetic field, but also to parameters like the initial inclination angle, the volume fraction of the particles, the shear strain and the ratio between the distance of two adjacent particles and the radius of the particles themselves.

### 3. Simulations

The proposed model has been used to analyze the influence of the initial tilt angle of the particle chain and the magnetic field on the magneto-induced shear storage modulus of the MRE. The particle size of 5μm used in this paper represents an example to illustrate the effect of the magnetic field and the orientation angle on this modulus. The parameters used are shown in Table 1.

**Table 1 Parameters of the model**

Parameter	Value
Constant (A)	1.082
Constant (C)	1.2
Volume fraction of CIP (φ)	0.27
Permeability of MRE (μ <sub>1</sub> )	1
Vacuum permeability (μ <sub>0</sub> )	4π×10 <sup>-7</sup> N/A <sup>2</sup>
Shear strain of MRE (γ)	0.1%
Radius of the particle (a)	5μm
Initial distance of adjacent particles (r <sub>0</sub> )	17μm

The values of the magnetic susceptibility under different magnetic fields are shown in Table 2.

**Table 2 Magnetic susceptibility under different magnetic fields**

mT	33	79	124	169	212	255
emu/g.Oe	0.0575	0.0556	0.055	0.0534	0.0512	0.0478
mT	298	340	381	421	461	500
emu/g.Oe	0.0447	0.0432	0.041	0.0387	0.037	0.035
mT	539	577	614	650	686	720
emu/g.Oe	0.033	0.0315	0.03	0.0286	0.0275	0.0265

mT	756	790	823	855	887	918
emu/g.Oe	0.0256	0.0247	0.0238	0.023	0.0222	0.0216
mT	949	978	1007	1036	1064	1089
emu/g.Oe	0.021	0.0205	0.0199	0.01947	0.019	0.0186

The magnetization of the carbonyl iron powder under magnetic field is nonlinear (Fig. 6).

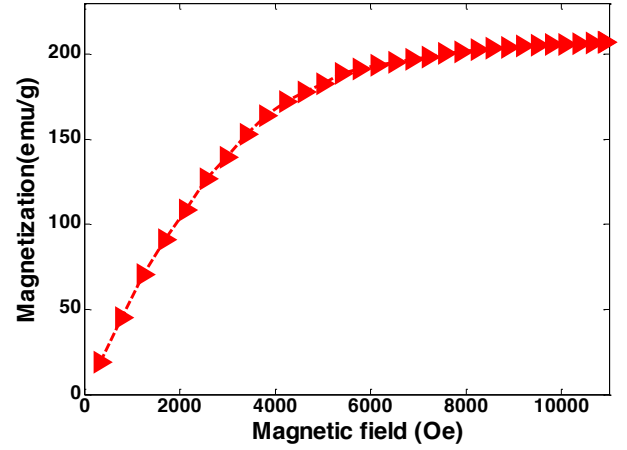


Figure 6 Magnetization curve of carbonyl iron powder [33]

The magneto-induced shear modulus with an initial inclination angle varying from 0° to 90° has been here calculated. Figure 7 shows the change of the magneto-induced shear modulus when the magnetic field varies from 0 to 1100mT.

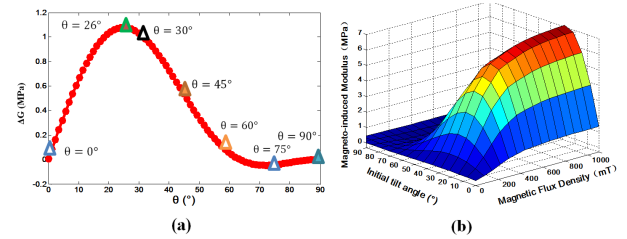


Figure 7 Simulation results (a) The variation of the magneto-induced modulus with the inclination angle of particle chain under the same magnetic field (b) Effect of the initial inclination angle of the particle chain and the magnetic field on the magneto-induced shear modulus

One can observe in Figure 7 that the magneto-induced shear modulus increases with the increase of the magnetic field and then tends to saturation; this is an obvious magnetorheological effect. The initial inclination angle of the particle chain has a significant influence on the magneto-induced shear modulus. When the initial tilt angle increases between 0 and 90°, the magneto-induced shear modulus increases and then decreases, reaching a maximum for an angle close to 26°. The rate of increase between 0 and 26° is higher than that the decrease one observed between 26 and 63°. The magneto-induced modulus is therefore most sensitive to the change of the tilt angle between 0 and 30°. When the initial tilt angle is greater than 63°, the value of the magneto-induced modulus of the MRE is negative, with

an absolute value first increasing, and then decreasing. It is worth pointing out that MREs under the same external magnetic field with a tilted chain between 0 and 63° exhibits in general improved magneto-induced properties and larger magneto-induced modulus than the elastomer without the tilted chain. The proposed model can only express the change trend of magneto-induced modulus with the orientation angle of particle chain, but cannot express the precise value of magneto-induced modulus.

In general, an interaction force between the magnetized particles is generated to resist the deformation when a sample of magneto-rheological elastomer is sheared by an external force under an external magnetic field. When the initial inclination angle of the particle chain increases, the interaction force against the shear deformation firstly increases, and then diminishes until the direction of the force changes. The value of the magneto-induced modulus therefore first increases, and then decreases depending upon the initial tilt angle. At large angles the value of the magneto-induced modulus can become negative; that implies that the magnetized particles within the matrix tend to move along the direction of the applied magnetic field under the shear deformation. Due to the constraining effect of the matrix at the interface with the particles, the displacement of the latter will cause stress concentrations in the matrix, with a resulting magneto-induced modulus appearing in the whole magneto-rheological composite.

#### 4. Experiments

Samples of MREs have been fabricated by using a silicone rubber matrix. Thirty different samples with various particle sizes (3-5 $\mu$ m, 10 $\mu$ m, 38 $\mu$ m, 75 $\mu$ m, 150 $\mu$ m, respectively) and different particle chains at initial inclination angles of 0°, 30°, 45°, 60°, 75°, 90° have been prepared. The dynamic viscoelastic properties of the samples were tested using rheometer.

##### 4.1 Fabrication of the MRE specimens

The materials of the MRE samples include a base polymer, a crosslinking agent, platinum catalyst and carbonyl iron powder (Table 3).

**Table 3 Materials used to prepare the magneto-rheological elastomers**

Materials	Brand
Polydimethylsiloxane	AXC103
Silicone oil	RH-H502
Platinum catalyst	VM-23
Carbonyl iron powder (CIP)	3~150 $\mu$ m

The preparation involves the use of a double planetary vacuum mixer, a magnetic adding device, and a temperature-

controlled drying box. A schematic diagram of the fabrication process used to produce the magneto-rheological samples is shown in Fig. 8.

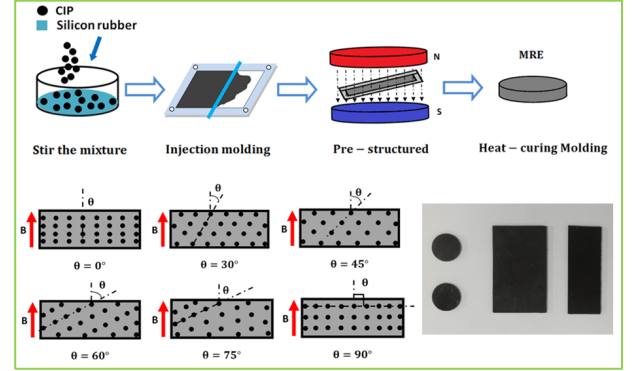


Figure 8 Preparation process of MRE

Quantities of carbonyl iron powder (wt 33.3%) and polydimethylsiloxane (wt 66.1%) have been stirred in a double planetary electric mixer for 10 min. Silicone oil (wt 0.4%) was then added and stirred for 10 min. A platinum catalyst (wt 0.2%) was added at the end. The whole mixture has been stirred for additional 10 min. During the stirring process, the internal part of the agitator was in vacuum to remove the bubbles in the mixture. The stirred homogeneous mixture was then injected into an aluminum mold. The mold was then placed in a uniform magnetic field environment generated by two permanent magnets to pre-structure the material architecture. The fixture with adjustable tilt angle is used to fix the mold in the magnetic adding device. The low viscosity of liquid rubber ensure that particles in MRE can be pre-structured into chains in an external magnetic field. MREs with different initial inclination angles of the particle chain have been prepared by adjusting the angle between the aluminum mold and the magnetic field. After pre-structuring the MRE samples have been fabricated by solidifying the samples in a drying chamber at a constant temperature of 75°C for about 3 hours.

Rubber with lower viscosity is usually used as matrix in magneto-rheological elastomers to let the magnetic particles forming chains during the pre-structure process. The use of internal field excitations is however a possible solution to fabricate thick specimens MRE specimens, or samples with general high viscosity matrix materials. The pre-structured magnetic field can be generated by internal excitations with distributed electrified coils in the matrix, which can control the orientation of the particles chain.

The internal microstructure of the samples has been characterized by a TM3030 Plus desktop scanning electron microscopy (SEM). The arrangement of the particles in the samples can be clearly observed (Figure 9).



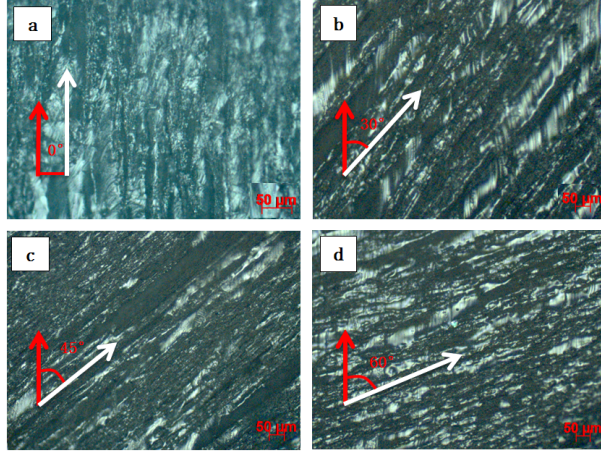


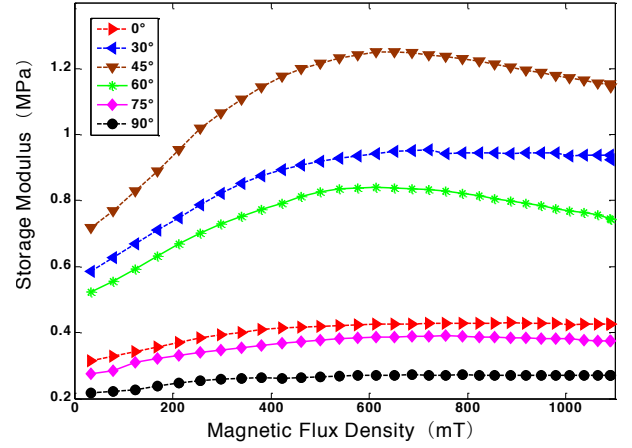
Figure 9 Microstructure of the MRE samples with particle chains of different initial inclination angles (The red arrow represents the direction of the applied magnetic field, while the white one indicates the direction of the particle chain)  
a. ( $0^\circ$ ) b. ( $30^\circ$ ) c. ( $45^\circ$ ) d. ( $60^\circ$ )

#### 4.2 Experimental setup

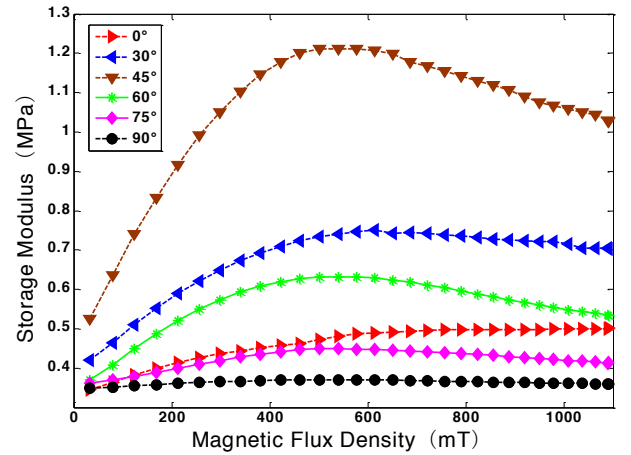
The dynamic mechanical properties of the MRE samples have been measured using rheometer (MCR301) in oscillating shear mode. The samples were cut into a disc with a thickness of 2 mm and a diameter of 20 mm, and placed on a platform under a variable magnetic field. The samples were also in contact with a parallel plate clamp. The angle between the external magnetic field and the internal particle chain of the MRE represents here the initial inclination of the particle chain. The rheometer tests have been carried out at 10 Hz, with a dynamic strain of 0.1% (shear strain of 0.1% is used to keep the samples of MRE in the linear viscoelastic region) and the compressive load of 5N.

##### 4.2.1 Shear storage modulus

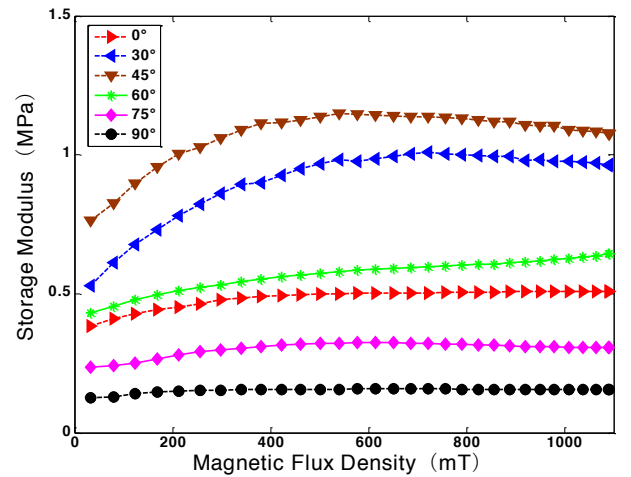
The shear storage modulus represents the value of the MRE modulus under a magnetic field. The results from the tests are shown in Figure 10. Increasing magnitudes of the magnetic field lead to a significant magneto-rheological effect on the specimens. As a general trend, the storage modulus of the samples first increases, and then decreases at constant magnetic field and with the increase of the initial inclination angle of the particle chain. The storage modulus follows this particular trend for every particle size considered in this work. The storage modulus shows also a maximum value when the initial inclination angle is  $45^\circ$ . The storage modulus of the samples at  $30^\circ$ ,  $45^\circ$ , and  $60^\circ$  inclination angle is larger than the modulus for the other configurations. This is a clear indication that the mechanical properties of the MRE could be tailored and improved by varying the initial tilt angle of the particle chain.



(a)

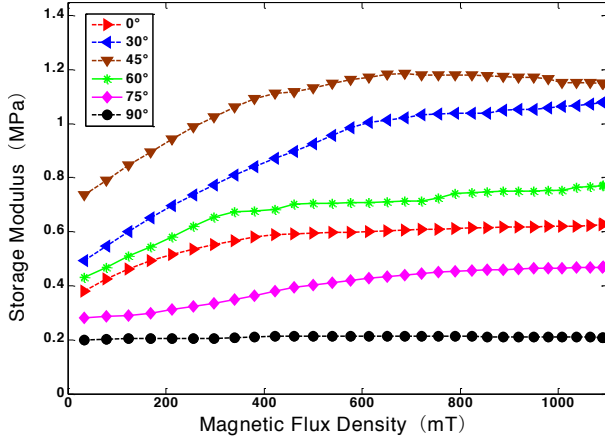


(b)

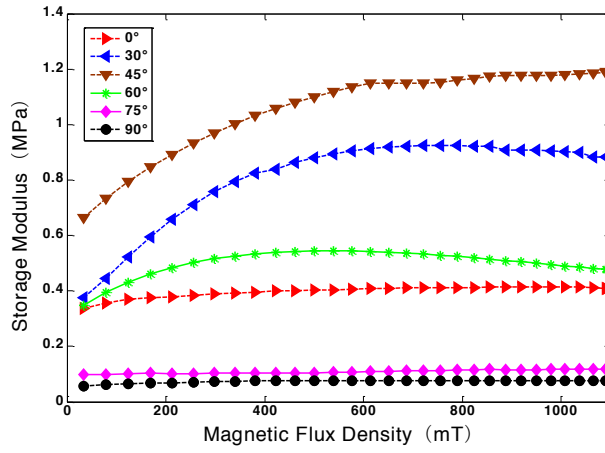


(c)





(d)

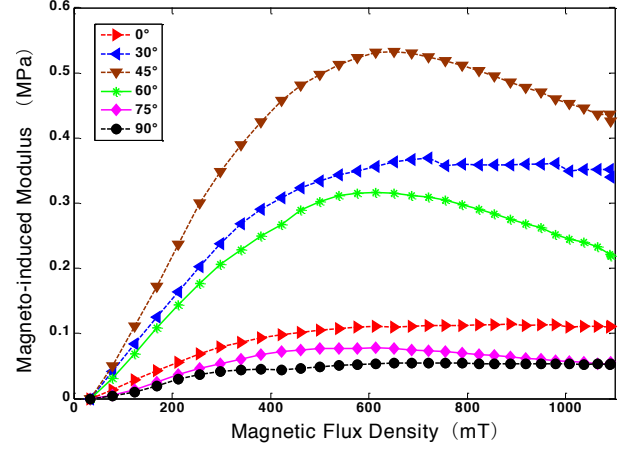


(e)

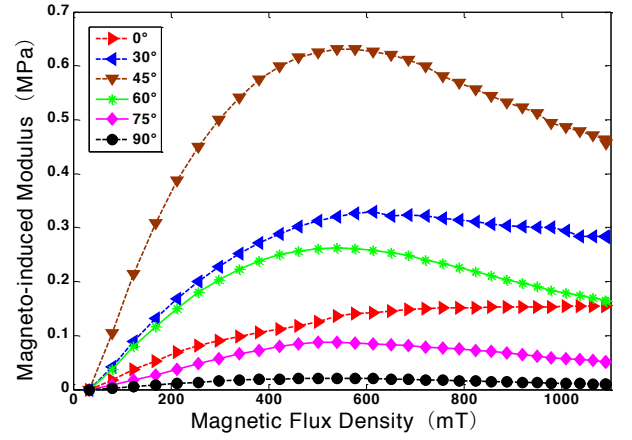
Figure 10 The variation of the storage modulus with the initial inclination of the particle chains under different magnetic fields. The particle sizes of the MRE samples are: (a) 3-5 $\mu\text{m}$  (b) 10 $\mu\text{m}$  (c) 38 $\mu\text{m}$  (d) 75 $\mu\text{m}$  (e) 150 $\mu\text{m}$ .

#### 4.2.2 Magneto-induced storage modulus

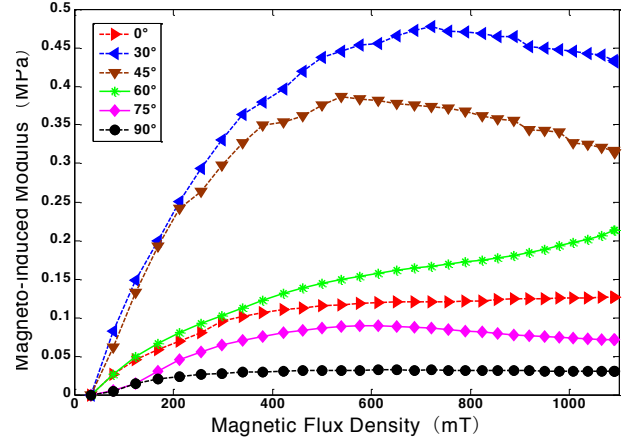
The magneto-induced modulus is the difference between the storage modulus and the zero-field modulus of MRE under a variable magnetic field.



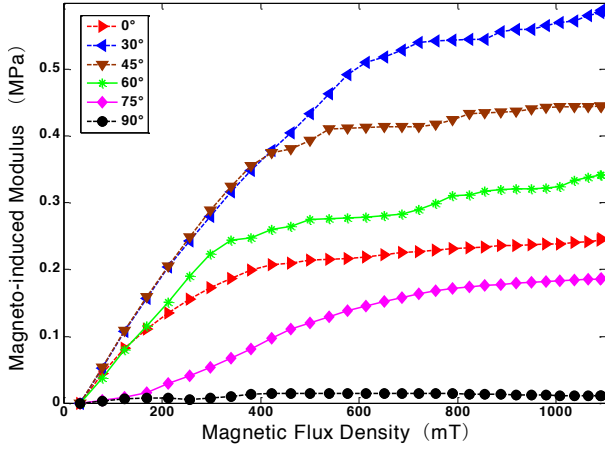
(I)



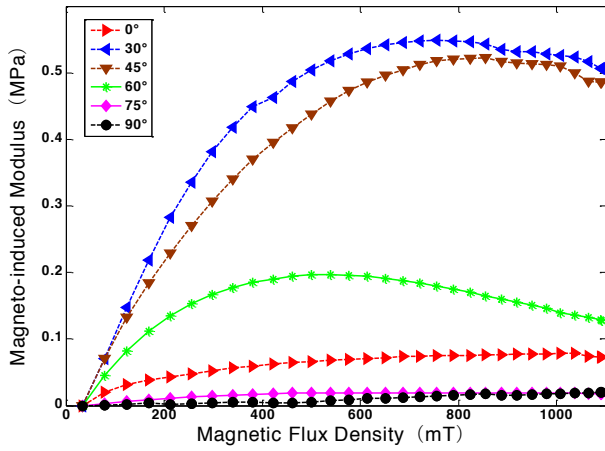
(II)



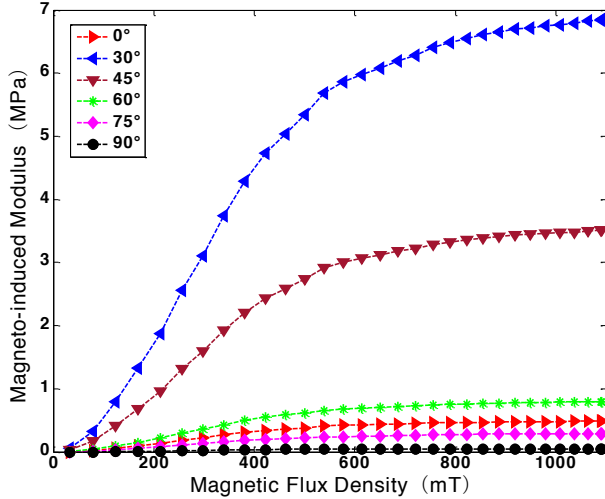
(III)



(IV)



(V)



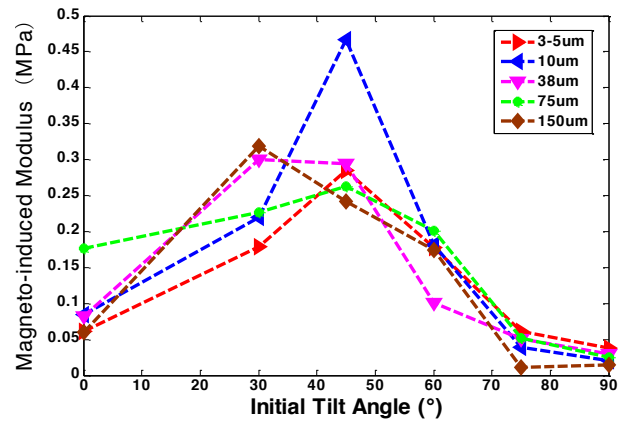
(VI)

Figure 11 The variation of the magneto-induced modulus with the initial inclination of the particle chains under different magnetic fields. The particle sizes are: (I) 3-5 $\mu\text{m}$  (II) 10 $\mu\text{m}$

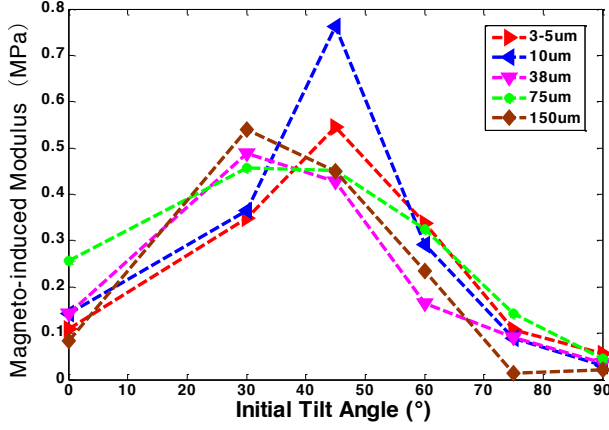
(III) 38 $\mu\text{m}$  (IV) 75 $\mu\text{m}$  (V) 150 $\mu\text{m}$  (VI) Theoretical simulation

The variation of the magneto-induced modulus with the initial tilt angle of the particle chain is shown in Fig. 11 (I~V). The simulation from the proposed theoretical model are consistent with the test results when the particle size is large (Fig. 11 (VI)). The results of the particle size at 38 $\mu\text{m}$ , 75 $\mu\text{m}$ , and 150 $\mu\text{m}$  are consistent with the trends predicted by model data. The magneto-induced modulus maximizes its value for an initial chain angle of 30°. The order of maximum values of the modulus versus the chain angle ( $90^\circ < 75^\circ < 0^\circ < 60^\circ < 45^\circ < 30^\circ$ ) is consistent with the findings of Boczkowska et al. [26]. The model provides a negative magneto-induced modulus at 75° in the simulation results. However, in the actual test, the rotation direction of the parallel plate of rheometer changes in a clockwise-counterclockwise harmonic manner under the oscillating shear mode, so the shear force can be considered to alternate from two different directions. The data measured in the text can be therefore considered as the absolute value of the magnetic induction modulus. At a smaller particle size, the value of the magneto-induced modulus at 45° is larger than at 30°, and the storage modulus of MRE at some tilt angles shows a decreasing trend at 600 mT and above; this may be due to the agglomeration of small particles that results in imperfections from the experimental results. When the particle size is 75 $\mu\text{m}$  the magneto-induced modulus and the magnetorheological effect of the sample with a 30° angle are 0.59MPa and 115% respectively. These values increase by 164% and 80% compared to the analogous ones from the sample with an inclination of 0. The experimental results clearly show that MREs possess a higher magneto-induced modulus and magnetorheological effect when the particle chain and the applied magnetic field have an initial tilt angle with 30°, 45°, 60°.

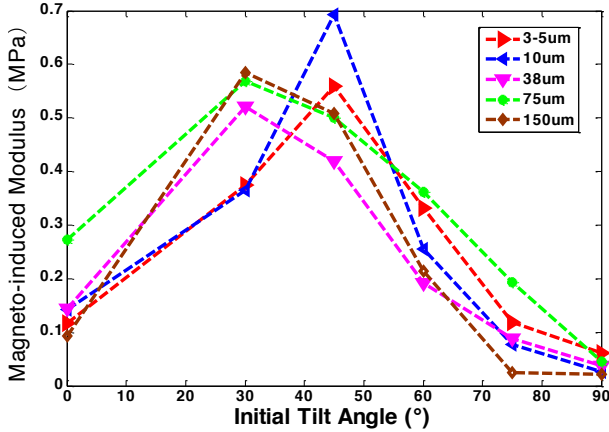
#### 4.2.3 The relationship between the particle size and the magneto-induced modulus



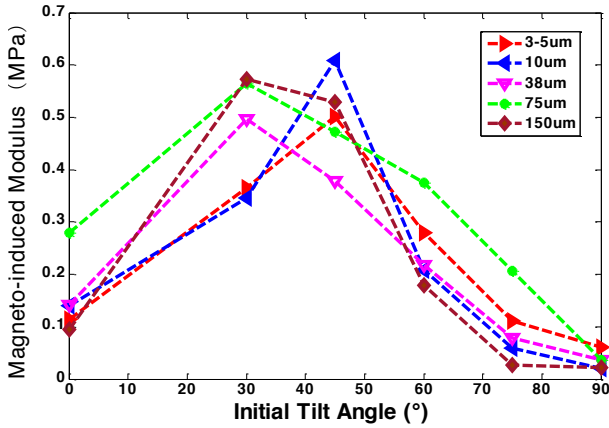
(a) 200mT



(b) 500mT



(c) 800mT



(d) 1000mT

Figure 12 Effect of the particle size on the magneto-induced modulus at different initial inclination angles. The applied magnetic fields are: (a) 200mT, (b) 500mT, (c) 800mT, and (d) 1000mT

The tests also show that the particle size has a large influence on the magneto-induced modulus. Figure 12 shows the effect of the particle size and the initial inclination on the magneto-induced modulus at different external magnetic fields. In the

proposed model, the magneto-induced modulus is proportional to the cubic power of the ratio of particle size to the initial distance between particles. When the initial tilt angle is  $0^\circ$ , the magneto-induced modulus of the samples first increases and then decreases with the increase of the particle size. The value of the magneto-induced modulus reaches a maximum when the particle size is  $75\mu\text{m}$ , which is consistent with Jin's findings [34].

The experimental results however do not show the same trend for other angles. When the initial tilt angle is  $30^\circ$ , the maximum value of the magneto-induced modulus of the sample is reached when the particle diameter is  $150\mu\text{m}$ . On the opposite, for the particle with a diameter of  $10\mu\text{m}$  this maximum value is reached for an initial tilt angle of  $45^\circ$ , and at an angle of  $60^\circ$  for a particle of  $75\mu\text{m}$  diameter. The reason behind this behavior is the fact that when the MRE samples is pre-structured, the thickness of the specimen is different when the particles are chained in the direction of the magnetic field; this significantly affects the initial distance between the particles. The relationship among particle chain size, initial distance, dip angle and magneto-induced modulus is a matter that would need further in-depth studies.

## 5. Conclusions

We provide in this work an explanation of the micromechanical interaction between particles in magneto-rheological elastomers based on the theory of magnetic dipoles and the magnetic field coupling between particles aligned in chains. The results of the model show that the magneto-induced shear storage modulus of the MREs has a strong dependence on the initial inclination of the internal particle chain. Silicone rubber-based MREs with different particle sizes and different initial inclination angles have been also prepared and their magneto-induced mechanical properties tested. The main conclusions of the work are as follows:

1. The mechanical properties of MREs depend not only on the properties of the matrix material and the particle content, but also on the arrangements of the internal particles. The model proposed in this paper can explain and predict the effect of the initial inclination angle of the particle chains on the magneto-induced properties of MRE. It also provides a theoretical design basis to explore the magneto-induced mechanism and the development of high-performance magnetorheological effect MREs.

2. The arrangement of the particle chains has a significant influence on the mechanical properties of the MREs. The storage modulus of the MRE has an increase/decrease dependence with the initial inclination angle between the particle chain and the applied magnetic field, and reaches a maximum at  $45^\circ$ . The initial modulus and the magneto-rheological effect of the MREs with inclinations of  $30^\circ$ ,  $45^\circ$  and  $60^\circ$  are larger than those with an inclination of  $0^\circ$ . This clearly indicates that one can effectively improve the magneto-induced mechanical properties of MREs by changing the initial inclination of the particle

chains. With a constant particle fraction, the magnetorheological effect of the MRE can also be significantly improved by changing the initial tilt angle of the particle chain.

3. The size of the particle has also a strong effect on the magneto-induced modulus of the MREs. By optimizing the particle size and the internal architecture, the magneto-induced properties of the MREs can also be improved to a large extent.

The model proposed here takes into account only the interaction between particles. Also, the idealized assumptions used here could lead to discrepancies between the experimental and simulation results. More realistic distributions and near-neighbouring interactions between particles should be fully considered in follow-up works.

## 6. Acknowledgments

The authors would like to thank Prof. Miao Yu and Dr. Song Qi for their help in data testing.

## 7. Funding

The research was supported by the Fundamental Research Funds for the Central Universities (JD1909). Jianfei Yao would like to thank Chinese Scholarship Council (CSC) for the funding of his research work. Jianfei Yao and Fabrizio Scarpa would like to acknowledge the support from the University of Bristol.

## 8. References

- [1] Ginder J M, Nichols M E, Eliea L D, and Tardiff J L 1999 Magnetorheological Elastomers: Properties and Applications *Part of the SPIE Conference on Smart Materials Technologies. California*. **3675** 131-138
- [2] Jolly M R, Carlson J D, Muoz B C 1996 A model of the behaviour of magnetorheological materials *Smart Materials and Structures*. **5(5)** 607-614
- [3] Yang Jian, Du Haiping, Li Weihua, et al 2013 Experimental study and modeling of a novel magnetorheological elastomer isolator *Smart Materials and Structures*. **22(3)** 117001-117014
- [4] Li Yancheng, Li Jianchun, Tian Tongfei, Li Weihua 2013 A highly adjustable magnetorheological elastomer base isolator for applications of real-time adaptive control *Smart Materials and Structures*. **22** 095020
- [5] J Yang, S S Sun, H Du, W H Li, G Alici and H X Deng 2014 A novel magnetorheological elastomer isolator with negative changing stiffness for vibration reduction *Smart Materials and Structures*. **23** 105023
- [6] Behrooz M, Wang X.J, Gordaninejad F 2014 Performance of a new magnetorheological elastomer isolation system *Smart Materials and Structures*. **23** 045014
- [7] Jian Yang, Shuaishuai Sun, Tongfei Tian, Weihua Li, Haiping Du, Gursel Alici and Masami Nakano 2016 Development of a novel multi-layer MRE isolator for suppression of building vibrations under seismic events *Mechanical Systems and Signal Processing*. **811** 70-71
- [8] Yu Tao, Rui X T, Yang F F, Chen G L, et al 2018 Design and experimental research of a magnetorheological elastomer isolator working in squeeze/elongation-shear mode *Journal of Intelligent Material Systems and Structures*. **29(7)** 1418-1429
- [9] Hyun Kee Kim, Hye Shin Kim and Young-Keun Kim 2017 Stiffness control of magnetorheological gels for adaptive tunable vibration absorber *Smart Mater. Struct.* **26** 015016
- [10] Anna Boczkowska and Stefan Awietjan 2012 Microstructure and properties of magnetorheological elastomers *Advanced Elastomers-Technology, Properties and Applications*. **(9)** 147-180
- [11] An, J. S., Kwon, S. H., Choi, H. J., Jung, J. H., & Kim, Y. G 2017 Modified silane-coated carbonyl iron/natural rubber composite elastomer and its magnetorheological performance *Composite Structures*. **160** 1020-1026
- [12] Ge L, Gong XL, Fan YC, Xuan SH 2013 Preparation and mechanical properties of the magnetorheological elastomer based on natural rubber/rosin glycerin hybrid matrix *Smart Materials and Structures*. **22(11)**: 115029
- [13] Miao Yu, Song Qi, Jie Fu, Pingan Yang, Mi Zhu 2015 Preparation and characterization of a novel magnetorheological elastomer based on polyurethane /epoxy resin IPNs matrix *Smart Materials and Structures*. **24**: 045009
- [14] A. Boczkowska & S. F. Awietjan 2011 Effect of the elastomer stiffness and coupling agents on rheological properties of magnetorheological elastomers *Materials Characterisation*. **V** 263-274
- [15] Gong, X., Zhang, X., Zhang, P 2005 Study of mechanical behavior and microstructure of magnetorheological elastomers *International Journal of Modern Physics B*, **19 (07n09)** 1304-1310
- [16] Boczkowska A, Awietjan S, Wroblewski R 2007 Microstructure property relationships of urethane magnetorheological elastomers *Smart Mater. Struct.* **16** 1924-1930
- [17] Vineet Kumar, Dong-Joo Lee Iron 2017 Particle and anisotropic effects on mechanical properties of magneto-sensitive elastomers *Journal of Magnetism and Magnetic Materials*. **441** 105-112
- [18] Zhu Xuli, Meng Yonggang, Tian Yu 2010 Effects of particle volume fraction and magnetic field intensity on particle structure of magnetorheological elastomers *Journal of Tsinghua University(Science and Technology)*. **2** 246-249
- [19] Jolly M R, Carlson J D 1996 The Magnetoviscoelastic Response of Elastomer Composites Consisting of Ferrous Particles Embedded in a Polymer Matrix *Journal of Intelligent Material Systems and Structures*. **7** 613-622
- [20] Davis L C 1999 Model of magnetorheological elastomers *Appl. Phys.* **85** 3348-3351
- [21] Shen Y, Golnaraghi M F, Heppler G R.z 2004 Experimental research and modeling of magnetorheological elastomers *Journal of Intelligent Material Systems and Structures*. **15(1)** 27-35
- [22] Zhu Juntao, Xu Zhaodong, Zhang Xiangcheng 2011 Main chain adsorption model of magnetorheological elastomer *Journal of Southeast University (Natural Science Edition)*. **2** 342-346
- [23] Suo Si, Xu Zhao dong, Xu Feihong 2016 A model of magnetorheological elastomer based on chi-square distribution *Journal of Functional Materials*. **47(9)** 9063-9067
- [24] Yu miao, Yan xiaorui, Xia Yongqiang 2009 Analysis on influencing factors of MR elastomer magneto-induced effect

- 
- based on chain-like model *Journal of Functional Materials*. **40(8)** 1263–1266
- [25] Anna Boczkowska, Stefan F. Awietjan 2009 Urethane Magnetorheological Elastomers – Manufacturing, Microstructure and Properties *Smart Materials for Smart Devices and Structures*. **154** 107–112
- [26] Boczkowska A, Awietjan SF, Pietrzko S, et al. Mechanical properties of magnetorheological elastomers under shear deformation *Composites Part B: Engineering*. **43(2)** 636–640
- [27] Tongfei Tian, Masami Nakano 2018 Fabrication and characterisation of anisotropic magnetorheological elastomer with 45° iron particle alignment at various silicone oil concentrations *Journal of Intelligent Material Systems and Structures*. **29(2)** 151–159
- [28] Gao Wei, Wang Xingzhe 2015 Model and analysis of magnetic Field-induced shear modulus of magnetorheological elastomer with tilted chain *China Science paper*. **4** 433–437
- [29] Hyoung Jin Choi 2008 Preparation and Electro-Thermoconductive characteristics of magnetorheological suspensions *International Journal of Modern Physics B*. **29** 5041–5064
- [30] D. Gignoux, J.C. Peuzin, Magnetostatics, in: É. du T. de Lacheisserie, D. Gignoux, M. Schlenker (Eds.) 2002 *Magnetism I—Fundamentals*, Kluwer Academic Publishers. 19–78
- [31] G. Diguët, E. Beaunon, J.Y. Cavaillé 2009 From dipolar interactions of a random distribution of ferromagnetic particles to magnetostriction *Journal of Magnetism and Magnetic Materials*. **321** 396–401
- [32] Dang H, Zhu YS, Gong XL, Zhang PQ 2005 Revised model of the magnetorheological elastomer based on distributed chains *Chinese Journal of Chemical Physics*. **18(6)** 971–975
- [33] Antonio J. F. Bombard, Marcelo K Nobel, Maria Regina Alcântara and Inês Joeke 2002 Evaluation of Magnetorheological Suspensions Based on Carbonyl Iron Powders *Journal of Intelligent Material Systems and Structures*. **7** 471–478
- [34] Qian Jin, Yong-gang Xu, Yang Di, Hao Fan 2015 Influence of the Particle Size on the Rheology of Magnetorheological Elastomer *Materials Science Forum*. 757–763